Fracture Failure Bodies of Porous Concrete (foam-like), Normal Concrete, Ultra-High-Performance-Concrete and of the Lamella - *generated on basis of Cuntze's Failure-Mode-Concept (FMC)*

Ralf Cuntze
D-85229 Markt Indersdorf, Matthaeus-Guenther-Str. 32, Ralf_Cuntze@t-online.de;
formerly MAN Technologie AG, Augsburg, Germany,
now linked to Carbon Composites e.V. (CCeV), Augsburg and CC-TUDALIT, Dresden

Abstract:

So-called fracture (failure) bodies are required to perform designing. The surface of such a fracture body of brittle behaving materials is determined by the points of all those stress states that lead to fracture.
In this paper the basic ideas of the underlying theory, Cuntze's Failure-Mode-Concept (FMC), are briefly presented. Then, the FMC-based strength criteria for a large variety of isotropic construction materials such as porous Concrete Stone, Normal Concrete, UHPC and for the transversely-isotropic carbon fiber-reinforced polymer Lamella are enlisted. Available multi-axial fracture test data were mapped to validate the generated fracture failure models. Eventually, for these materials fracture bodies and distinct cross–section of them, principal stress planes, octahedral stress planes and meridian planes, are displayed.

1. Introduction

The wide variety of new materials in engineering requires the knowledge of the fracture state in order to enable verification of the designed structural part. And this much more since lightweight design requires a higher exertion of the material and thereby contributes to sustainable engineering. Applicable fracture (failure) bodies are searched to perform this. The surface of such a fracture body of a brittle behaving material is determined by the points of all those stress states that lead to fracture.
Experience shows: (1) similarly behaving materials possess the same shape of a fracture body; (2) its size is fixed by the different tensile and compressive strengths. The author uses this knowledge together with his 3D- Failure Mode Concept which was successful in the twenty years lasting World-Wide-Failure-Exercises–I and –II on transversely-isotropic (UD) uni-directional fiber-reinforced composites. His concept leads to a desired simple Mises-like equivalent stress formulation for each mode of the isotropic concrete matrices and also for the UD lamella and sheet (≡ lamina or ply). In the case of isotropic materials 2 fracture modes are distinguished: Normal Fracture NF (tension) and Shear Fracture SF (compression). In the case of the lamella 5 fracture modes exist: 2 Fiber Fracture modes (FF under tension NF and compression SF) and 3 Inter Fiber Fracture modes (IFF1 under tension ≡ NF, IFF2 under compression ≡ SF and IFF3 under in-plane shear). Of course, modal formulations are to interact by an equation that captures the joint failure system with all its damaging activating

modes. On the surface of the fracture body the total 'material stressing effort' *Eff* with contributions from all activated modes *Eff* ^{modes} becomes *Eff* = 100% or the reserve factor *RF*= 1, [Cun16b].
In concurrent engineering the involved technical disciplines analysis and simulation are recognized as key enablers to increase competitiveness of new construction materials. However, the thereby applied tools must give confidence to the designer [Cun16c]. The FMC tool shall fulfil this desire.

2. Theoretical Background of Cuntze's Failure-Mode-Concept (FMC)

2.1 Basic knowledge from former investigators

Following Beltrami and Hencky-Mises-Huber, each invariant term or a multiple of it in the *strength failure function or strength criterion,* described by *F,* may be dedicated to one physical mechanism in the solid or cubic material element, respectively. Further, these mechanisms are linked to energies, namely: I_1^2 ~ dilatational energy from a volume change, J_2 ~ distortional energy from a shape change. What is missing in the case of compression-loaded materials is the Mohr-Coulomb-linked friction energy which is captured for the respective so-called pressure-sensitive materials by I_1.

2.2 Use of material symmetry and further experience

Under the presumption 'homogeneity is a valid assessment for the concerned material', regarding the respective tensors, it follows from material symmetry: *The Number of strengths ≡ number of elasticity properties! This means, a characteristic number of quantities is fixed: 2 for isotropic material and 5 for the transversely-isotropic UD lamina (≡ lamellas and sheets in civil engineering), see Table 1*. Hence, the applicability of material symmetry involves that a *minimum number of properties needs to be measured only* (cost + time benefits)! Therefore, material symmetry requirements are helpful when setting up strength criteria and test programs.

Table 1: FMC basics

1 If a material element can be homogenized to an ideal (= frictionless) crystal, then, material symmetry demands for the transversely-isotropic UD-material - 5 *elastic 'constants' E, ν ; 5 strengths R; 5 fracture toughnesses* K_c and - *2 physical parameters (such as CTE, CME, material friction value* μ *etc.)* *(for isotropic materials the respective numbers are 2 and 1)*
2 Mohr-Coulomb requires for the real crystal another inherent parameter, - the *physical parameter 'material friction' : UD* $\mu_{\perp\parallel}$, $\mu_{\perp\perp}$ *isotropic* μ
3 Fracture morphology witnesses: - Each strength corresponds to a distinct *failure mode* and to a *fracture type* as Normal Fracture (NF) or Shear Fracture (SF).

Again, comparing material behavior shows: (1) similarly behaving materials possess the same shape of a fracture body; (2) its size is given by the different (ultimate) tensile and compressive strengths. This will be applied for the Concrete Stone, lacking of test data.

2.3 Equivalent stress, multi-fold failure and mapping requirements

Idea of a modal equivalent stress for NF and SF:

For the failure mode Yielding the HMH hypothesis delivers an equivalent stress and this for all stress situations (normal stress, shear stress, torsion stress) when yielding comes to act. Similar to the (modal) HMH equivalent stress it is related to the material stressing effort

$$Eff^{Mises} = \sigma_{eq}^{Mises}/R_{po.2} \Rightarrow Eff^{fracture\ mode} = \sigma_{eq}^{fracture\ mode}/R_m\ ,\ Eff^{mode} = \sigma_{eq}^{mode}/\overline{R}^{mode}\ .$$

Above possibility to formulate equivalent stresses caused Cuntze to differentiate Global from Modal strength criteria types. About details and the Pros and Cons, see [Cun16c].

Capturing multi-fold failure effects:

The existence of twofold and threefold failure effects must be considered:

- A usual SFC just describes a 1-fold occurring failure mode or mechanism
- A multi-fold occurrence of a failure with its joint probabilistic effects must be additionally considered in the formulas as follows: *2-fold* $\sigma_{II} = \sigma_I$ tension or compression is elegantly solved by using J_3 ; *3-fold* $\sigma_{II} = \sigma_I = \sigma_{III}$ hydrostatic compression, by a closing bottom in the case of porous materials
  The 120°-located dents of the failure body, as the probabilistic result of the *2-fold* acting of the same failure mode, are usually described by replacing J_2 by $J_2 \cdot \Theta\,(J_3, J_2)$. It causes the non-circularity of the 120° rotational-symmetric isotropic fracture body.

Mapping requirements:

Available 2D test data sets must be mapped by the 3D failure function *F* in the 2D principal plane, and 3D test data sets on the 3D failure body or surface. Meridional shape (cross section of the failure body) functions should be not the result of a 2D meridional mapping of the associated test data, but the result of the meridian angle ϑ inserted into the 3D *F*.

3. Application of the Failure-Mode-Concept

3.1 Enlisting of FMC-derived Strength Criteria for Isotropic Materials

As well known, the HMF yield surface (body) is a cylinder, and builds a circular shape of the so-called π-plane or I_1 = constant plane, see *Fig.1* and *2*. For brittle behaving materials 'dents'

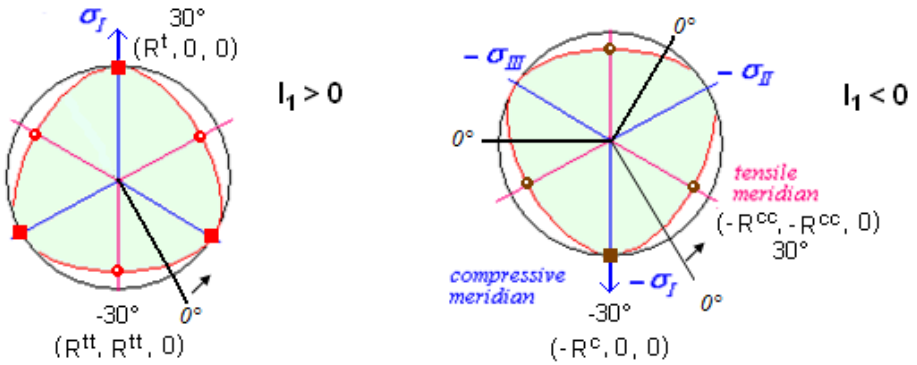

Figure 1: Mises cylinder shape, meridians, dents and meridian (,Lode stress) angles ϑ° around the 120°-hoop. Here, Ansatz sin(3ϑ) at 0° shear meridian taken

occur. *Table 1* contains all those strength criteria that lead to a non-circular shape of the π-plane. The indexes σ, τ mark the macroscopically responsible failure stress, Θ marks the non-circularity (roundness). In the formulas invariants are used and a non-circularity function Θ which is zero for circular shapes:

$$I_1 = (\sigma_I + \sigma_{II} + \sigma_{III})^T = \; f(\sigma) \;, \quad 6J_2 = (\sigma_I - \sigma_{II})^2 + (\sigma_{II} - \sigma_{III})^2 + (\sigma_{III} - \sigma_I)^2 = \; f(\tau)$$

$$27J_3 = \; (2\sigma_I - \sigma_{II} - \sigma_{III}) \cdot (2\sigma_{II} - \sigma_I - \sigma_{III}) \cdot (2\sigma_{III} - \sigma_I - \sigma_{II})$$

$$\Theta = \; \sqrt[3]{1 + d \cdot \sin(3 \cdot \vartheta° \cdot \pi / 180°)} = \sqrt[3]{1 + d \cdot 1.5 \cdot 3^{0.5} \cdot J_3 \cdot J_2^{\,-1.5}} \quad \text{with} \quad 0 < |d| < 0.99 \; .$$

Table 1: FMC-based 3D strength criteria for isotropic materials with consideration of the 120°-symmetric non-circular shape of the π-plane. F:= fracture failure condition (strength criterion), t:=tension, c:= compression, CrF:= crushing fracture

Normal Fracture *(deformation poor) I_1>0, hyperbola shape (= straight line in σ_{II} (σ_I)-diagram)*

$$F^{NF} = c_{NF\Theta} \cdot \frac{\sqrt{4J_2 \cdot \Theta_{NF} - I_1^{\,2}/3} + I_1}{2 \cdot \overline{R}^t}, \quad Eff^{NF} = c_{NF\Theta} \cdot \frac{\sqrt{4J_2 \cdot \Theta_{NF} - I_1^{\,2}/3} + I_1}{2 \cdot \overline{R}^t} = \; \sigma_{eq}^{NF} / \overline{R}^t$$

$c_{NF\Theta}$, $d_{NF\Theta}$ from the two points (R^t, 0,0) and (R^{tt}, R^{tt},0) or minimum error fit, if data available

Shear Fracture, dense *(shape + friction) I_1<0, paraboloid body shape, open bottom failure surface*

$$F^{SF} = c_{1SF\Theta} \cdot \frac{3J_2 \cdot \Theta_{SF}}{\overline{R}^{c\,2}} + c_{2SF\Theta} \cdot \frac{I_1}{\overline{R}^c} = \; 1, \quad Eff^{SF} = \frac{c_{2SF\Theta} \cdot I_1 + \sqrt{(c_{2SF\Theta} \cdot I_1)^2 + 12 \cdot c_{1SF\Theta} \cdot 3J_2 \cdot \Theta_{SF}}}{2 \cdot \overline{R}^c} = \sigma_{eq}^{SF} / \overline{R}^c$$

with $c_{2SF\Theta} = (1 + 3 \cdot \mu)/(1 - 3 \cdot \mu)$, $c_{1SF\Theta} \cdot \sqrt[3]{1 - d_{SF\Theta}} = 1 + c_{2SF\Theta}$ from ($-R^c$,0,0), $d_{SF\Theta}$ from ($-R^{cc}$,$-R^{cc}$,0)

and $\mu = \cos(2 \cdot \theta_{fpc}^{o} \cdot \pi / 180^o)$ from fracture angle θ_{fpc} : 45° (μ=0), 50° (μ= 0.174), .. or (see[Pet16]). For design purposes: 0 < μ < 0.3, the smaller value is on the conservative side

Crushing fracture, porous *(shape + volume) I_1 >=<0, pear shape, closed bottom surface, $\mu \approx 0$*

$$F^{CrF} = c_{CrF\Theta} \cdot \frac{\sqrt{4J_2 \cdot \Theta_{CrF} - I_1^{\,2}/3} - I_1}{2 \cdot \overline{R}^c} = 1, \quad Eff^{CrF} = c_{CrF\Theta} \cdot \frac{\sqrt{4J_2 \cdot \Theta_{CrF} - I_1^{\,2}/3} - I_1}{2 \cdot \overline{R}^c} = \sigma_{eq}^{CrF} / \overline{R}^c$$

$c_{NCrF\Theta}$, $d_{CrF\Theta}$ for $I_1 > 0$ from (R^t, 0,0), (R^{tt}, R^{tt},0) and for $I_1 < 0$ from ($-R^c$,0,0), ($-R^{cc}$,$-R^{cc}$,0)

SFV fracture *(shape + friction + volume), I_1 < 0, pear body shape, closed bottom failure surface (for instance for UHPC in the high hydrostatic pressure domain, about $I_1 / (\sqrt{3} \cdot R^t) < -10$) transition versus a global SFC since the failure mechanism changes. Considering all 3 mechanisms in the approach:*

$$F^{SFVF} = c_{1SFVF} \cdot \frac{3J_2 \cdot \Theta_{SFVF}}{\overline{R}^{c\,2}} + c_{2SFVF} \cdot \frac{I_1}{\overline{R}^c} + c_{3SFVF} \cdot \frac{I_1^{\,2}}{\overline{R}^{c\,2}} = \; 1, \quad Eff^{SFVF} = ...$$

determining the 4 unknowns by a mathematical fit (when mapping test data) or in design *engineering-like* - as above - by inserting ($-R^c$,0,0), ($-R^{cc}$,$-R^{cc}$,0), ($-R^{ccc}$,$-R^{ccc}$,$-R^{ccc}$) (∞, if open surface: in practice considered by a very high R^{ccc}) and one more characteristic point (see *Fig.8*) or a guess of the friction value μ.

Finally, interaction is performed according to

$$Eff \;\; = [(Eff^{NF})^m + (Eff^{SF})^m]^{m^{-1}} \quad \text{or} \quad Eff \;\; = [(Eff^{NF})^m + (Eff^{CrF})^m]^{m^{-1}} \quad \text{or} \quad ...$$

3.2 Pecularities with Fracture Bodies

Closures: *MaxI₁* and *minI₁* are the ends of a closed fracture body on the hydrostatic axis or I_1-axis of a brittle behaving material. *maxI₁* must be assessed whereas *minI₁* can be measured in the case of porous material. Both these points are firstly the result of a 3-fold acting Failure Mode.

Cap point, $I_1 > 0 : (\bar{R}^{ttt}, \bar{R}^{ttt}, \bar{R}^{ttt}) \rightarrow maxI_1 = 3 \cdot \bar{R}^{ttt}$

$\bar{R}^{ttt}$ not measurable. Estimation (due to Awaji, [Cun04]) via measured values $\bar{R}^{t}$, $\bar{R}^{tt}$

$$\bar{R}^{ttt} = \bar{R}^{t} / \sqrt[M]{3} \quad \text{with} \quad M = \ln(2) / \ln(\frac{\bar{R}^{t}}{\bar{R}^{tt}}) .$$

Bottom point, $I_1 < 0 : (-\bar{R}^{ccc}, -\bar{R}^{ccc}, -\bar{R}^{ccc}) \rightarrow minI_1 = -3 \cdot \bar{R}^{ccc}$ (closed body)

Fracture test data obtainable for *porous* solids (crushing fracture CrF) such as foam, nesting UD material, grey cast iron, concrete. For the brittle behaving materials, addressed above, an Awaji-based estimation looks reasonable and was applied.

- open fracture body : *Glass, Grey cast iron, Normal concrete, UHPC*
  (due to Poisson effect, concrete may NF-fracture under (bi-axial) 2D-compression)
- closed fracture body: *foam, 'concrete stone', Fiber-Reinforced-Plastic (FRP)*
  (even the fiber may NF-fracture under 3D-compression!).

The formulas for the cap and the bottom read

$$\frac{I_1}{\sqrt{3} \cdot \bar{R}^{t}} = s_{cap} \cdot (\frac{\sqrt{2J_2 \cdot \Theta_{NF}}}{\bar{R}^{t}})^2 + \frac{\max I_1}{\sqrt{3} \cdot \bar{R}^{t}}, \quad \frac{I_1}{\sqrt{3} \cdot \bar{R}^{c}} = s_{bot} \cdot (\frac{\sqrt{2J_2 \cdot \Theta_{CrF}}}{\bar{R}^{c}})^2 + \frac{\min I_1}{\sqrt{3} \cdot \bar{R}^{c}} .$$

The slope parameters s_{cap}, s_{bot} are determined by insertion of the respective hydrostatic strength point together with the associated point on tensile and compressive meridian.

Reduction of non-circularity with increasing $|I_1|$: From investigations of test results it is known that the non-circularity will reduce with increasing hydrostatic pressure $p_{hyd} = I_1/3$. Cuntze interprets this as an increasing redundancy effect. The flaws in the material do not more have the micromechanical damaging effect anymore under a compressive 3D stress state. This means, some sort of a healing occurs. Such a non-failure mode associated effect must be separately considered by a correction that takes into account whether the bottom is closed or not. A formula f_{I1}, regarding this effect is introduced ($d \Rightarrow D$) into

$$\Theta(I_1) = \sqrt[3]{1 + D \cdot f_{I1} \sin(3 \cdot \vartheta° \cdot \pi / 180°)}, \quad f_{I1} = \alpha \cdot \beta \cdot I_1^{\beta-1} \cdot \exp(-\alpha \cdot I_1^{\beta}) .$$

The same seems to be the case for $I_1 > 0$. The two by two parameters are determined by inserting the bi-axial strengths point I_1^{tt} , I_1^{cc} and assuming a decay of 50% at $2 \cdot I_1^{tt}$, $2 \cdot I_1^{cc}$.

4. Work Cases

4.1 Concrete Stone (foam-like), 'non-circular' without decaying circularity

Due to the analogy in material behavior '*porous concrete stone should behave similarly to porous foam'* the failure criteria for foam can be applied to a concrete stone, see *Fig.2* and data [Cun16a]. A concrete stone fracture body will be just larger due to its larger strengths.

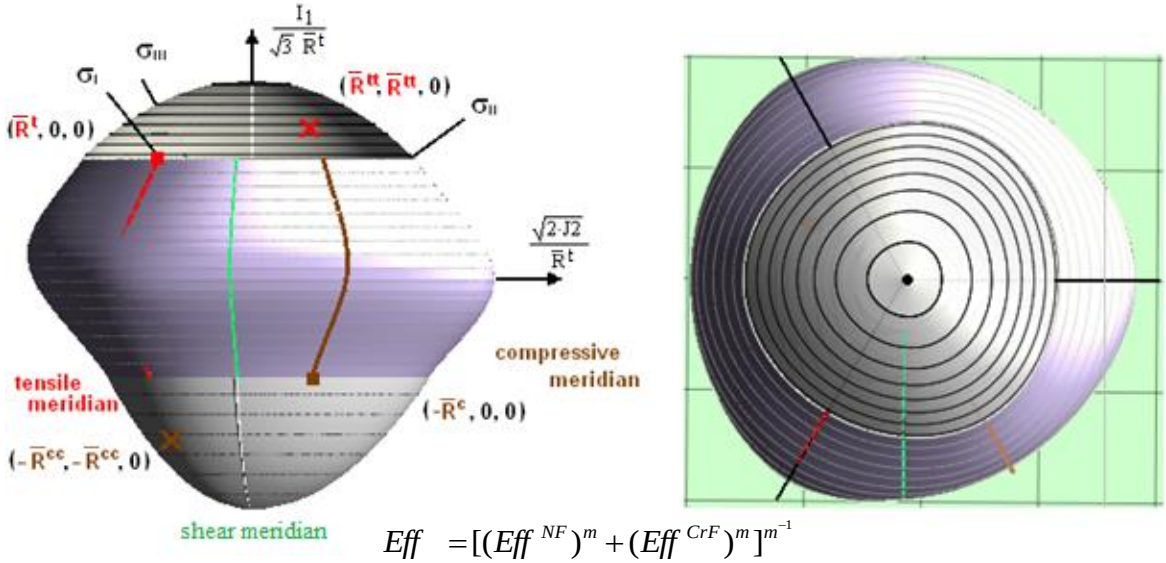

$$Eff = [(Eff^{NF})^m + (Eff^{CrF})^m]^{m^{-1}}$$

Figure 2: Fracture body of a porous concrete stone with its different meridians (left) and view from top (right). R:= strength $\equiv f$, $t := tensile, c := compressive$. *bar over means mean value,* J_2 *:='Mises'- invariant,* I_1*:= sum of principal stresses.(Mathcad plot. Test data, courtesy V. Kolupaev, LBF).* s_{cap}= -0.56, s_{bot}=1.09, d_{NF}, d_{CrF} = 0.17,- 0.55, $c_{NF\Theta}$, $c_{CrF\Theta}$ = 0.98, 0.95

*4.2 **Normal Concrete,** 'non-circular' with $|I_1|$-decaying circularity*

Necessary input data set for $I_1(R^t,0,0) > I_1 > \approx I_1(-2R^c, 0,0)$:

- For design engineering the following input is required: R^t, R^c, μ, d_{NF}, d_{SF}, m.
- Friction value: $0 < \mu < 0.3$, smaller value is on conservative side. Θ_{fp}= 51° (μ= 0.21)
- Interaction exponent: $0 < m < 0.3$, a smaller value is on the conservative side.

$\bar{R}^t = 4$ MPa, $\bar{R}^c = 40$ MPa, $\bar{R}^{tt} = 0.8 \cdot \bar{R}^t$ (assumed), $\bar{R}^{cc} = 51$ MPa, $\bar{R}^{ccc} = 1000$ MPa (set)

$M^t = \ln(2)/\ln(\bar{R}^t/\bar{R}^{tt}) = 3.11$, $\bar{R}^{ttt} = \bar{R}^t/3^{1/Mt} = 2.8$, $\max I_1 = 3 \cdot \bar{R}^{ttt} = 8.4$ MPa

Meridian: $c_{NF\Theta}$=0.96, $c_{1SF\Theta}$, $c_{2SF\Theta}$ = 6.48, 4.32; *NF:* α, β = 0.55, *1.9; SF:* α, β = 0.003, *1.92*
π-shape parameters : D_{NF} = 0.79, D_{SF} = 17 *(are related to d, but other mapping)*
Cap of the fracture body : s_{cap}= -0.85, *Interaction exponent: m* = 2.6.

Fig. 3 displays a bias cross-section of the Normal Concrete fracture body which means the shape of its principal stress plane.

Fig. 4 displays the octahedral stress plane , the horizontal cross-section or shape of the hoop plane, respectively. In this plot meridian-associated points are marked.

Fig. 5 completes with showing meridian cross-sections of the fracture body. As coordinates Lode-Haigh-Westergaard coordinates are used which equally count in all directions of the 3D stress space. The plot shows the chosen cap profile, the hyperbolic mapping of the NF domain, the paraboloid mapping of the SF domain and the transition zone. A yielding failure surface (in *Fig.5* the Mises cylinder) is terminated by a fracture failure surface!

Fig.6, eventually presents test data on the tensile meridian (points x) and the full set of test data (points o), located at different meridian angles ϑ in the 120° hoop section. Tensile meridian curve (left, red, ϑ = 30°), compressive meridian curve (brown, ϑ = -30°) and shear meridian curve (green, ϑ = 0°) are outlined. These meridian curve shapes are not the result of

a meridional mapping but result from the insertion of the respective meridian angle ϑ into the general 3D fracture body function.

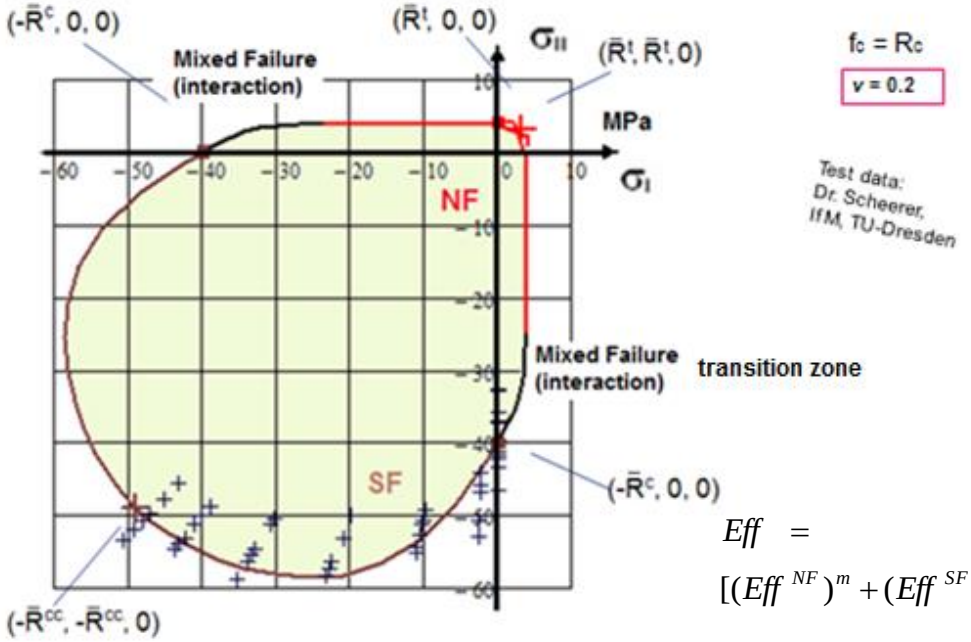

$$Eff = [(Eff^{NF})^m + (Eff^{SF})^m]^{m^{-1}} = 1$$

Figure 3: Normal Concrete, mapping of 2D-test data in the Principal Stress Plane. R:= strength $\equiv f, t:=$ $tensile, c:=$ $compressive$; *bar over means mean value. (Test data, courtesy S. Scheerer, IfM Dresden)*

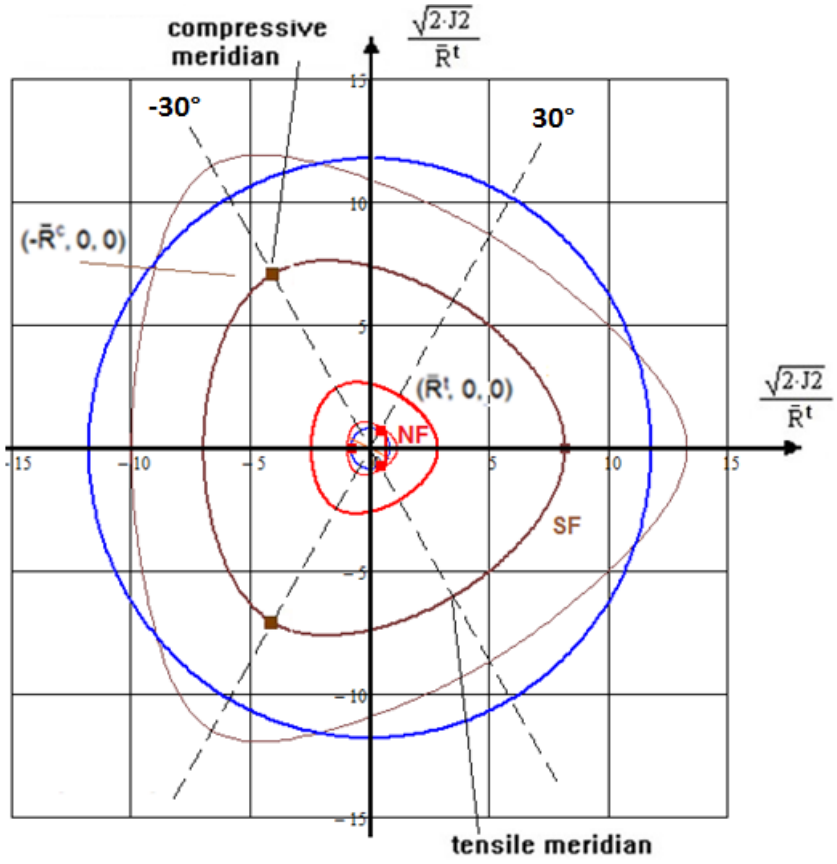

Figure 4: Octahedral stress plane or π-plane

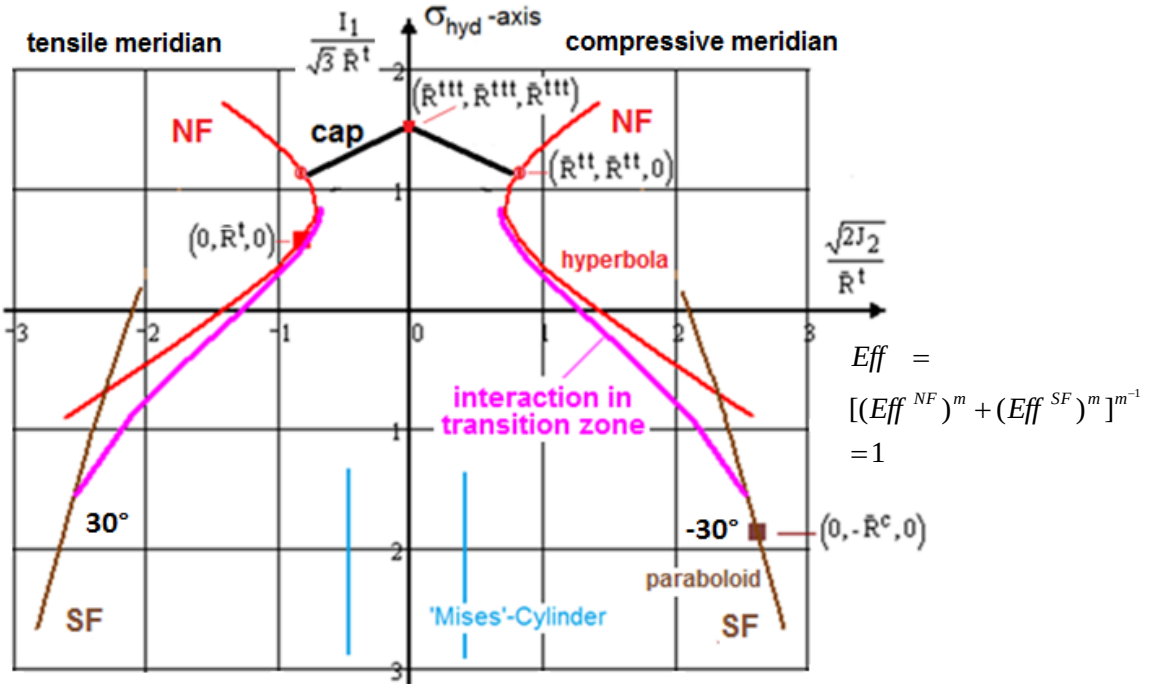

Figure 5: Visualization of the mode mapping functions and the meridian cross sections of the fracture body after interaction

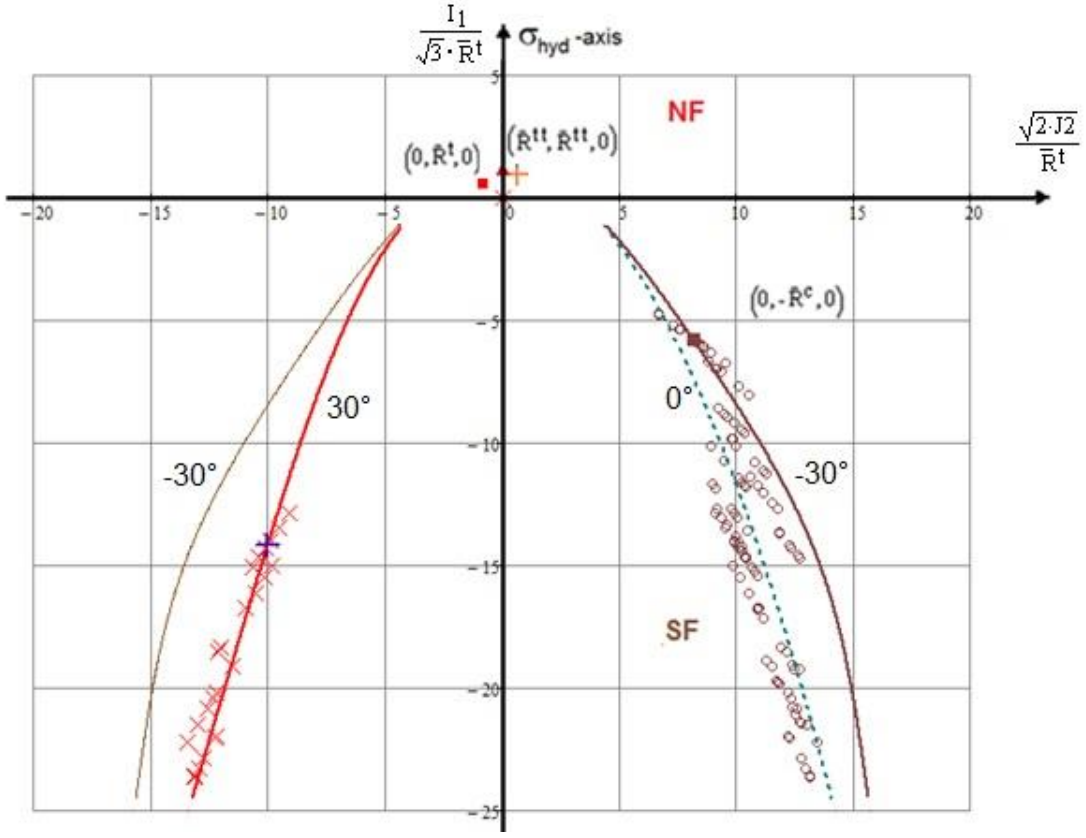

Figure 6: Tensile meridian (x, 30°), compressive meridian (-30°), and test data on the hoop ring (o, any 9, to indicate they are lying on a distinct hoop ring at different meridian angles 9)

Fig.7 depicts the fracture body indicating the three most interesting meridians. As specific points uniaxial strength and biaxial strength are marked. The body possesses inward dents for $I_1 > 0$ and outward dents for $I_1 < 0$ in contrast to porous concrete stone. These dents become

smaller with increasing $|I_1|$. Due to the Poisson effect it should be checked whether the material may tensile fracture (NF) under biaxial compression, $\varepsilon_{axial} > \max\varepsilon$.

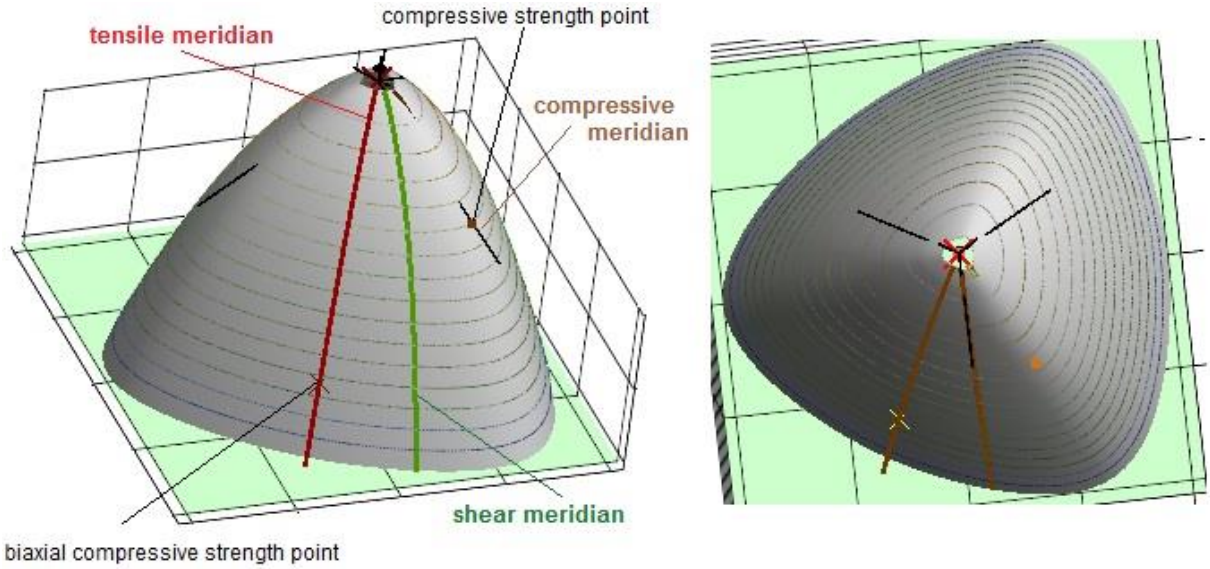

Figure 7: Fracture body of a normal concrete with its different meridians. maxI_1 = 8.4 MPa (Mathcad plot)

4.3 UHPC, 'non-circular' 'non-circular' with $|I_1|$-decaying circularity

Ultra-High-Performance-Concrete principally behaves similarly to Normal Concrete unless the normalized hydrostatic compression does not become larger than $|I_1/ R^t\cdot\sqrt{3}| \approx 10$ (> 300 MPa), see *Fig.10*. From about this stress state on a different failure behavior takes places, which can be substantiated best by the following test result: *Just a slight hydrostatic pressure of 6 MPa (N/mm²) increases the uniaxial strength capacity from 160 MPa up to 230MPa - 6 MPa = 224 MPa!* This explains why for the less 'dense' Normal Concrete R^{cc}/R^c is higher.

$$\sigma_{bruch} = (\sigma_I,\ \sigma_{II},\ \sigma_{III})_{bruch}^{T} : (-160,\ 0,\ 0)^T \Rightarrow (-230,\ -6,\ -6)^T$$

The author dedicates this to the still mentioned 'healing' effects. Since SF is not the only failure mode anymore, F^{SF} will be replaced by F^{SVF} to capture all effects

$$F^{SF} = c_{1SF\Theta}\cdot\frac{3J_2\cdot\Theta_{SF}}{\overline{R}^{c\,2}} + c_{2SF\Theta}\cdot\frac{I_1}{\overline{R}^c} \Rightarrow F^{SVF_h} = c_{1SFV}\cdot\frac{3J_2\cdot\Theta_{SF}}{\overline{R}^{c\,2}} + c_{2SFV}\cdot\frac{I_1}{\overline{R}^c} + c_{3SFV}\cdot\frac{I_1^{\,2}}{\overline{R}^{c\,2}}\ ,$$

engineering-like. Points for the determination of the SFV curve are indicated in *Fig.10*. By the way, for fiber-reinforced plastics a similar redundant behaviour occurs, see [Cun13, 14]. Again, mind the Poisson effect. The effortful calculation of the fracture body is in progress.

4.4 Lamella, Sheet (tape)

The UD invariants read [Cun04, 13, 14, 16c, Kad13, VDI2014]

$$I_1 = \sigma_1,\ I_2 = \sigma_2 + \sigma_3,\ I_3 = \tau_{31}^2 + \tau_{21}^2,\ I_4 = (\sigma_2 - \sigma_3)^2 + 4\tau_{23}^2,\ I_5 = (\sigma_2 - \sigma_3)(\tau_{31}^2 - \tau_{21}^2) - 4\tau_{23}\tau_{31}\tau_{21}.$$

After the replacement of the UD-invariants by the stresses they are composed of and after some simplifications with re-formulations to by-pass numerical solution problems the FMC-

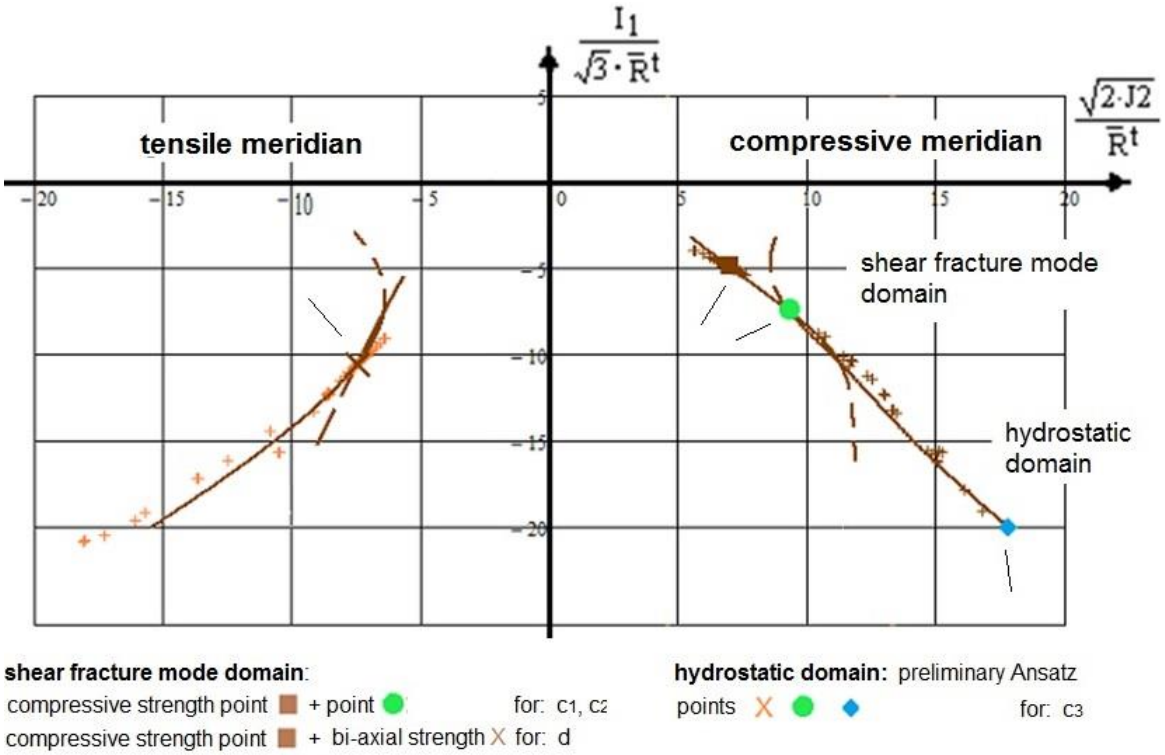

Figure 8: Ultra-High-Performance-Concrte (UHPC). (Test data, courtesy K.Speck, IfM Dresden)
$\bar{R}^t = 20$ MPa, $\bar{R}^c = 160$ MPa, $\bar{R}^{tt} = 0.89 \cdot \bar{R}^t$ (assumed), $\bar{R}^{cc} = 175$ MPa

based set of 5 strength criteria for this fiber-reinforced plastic material – embedded in a concrete matrix - is given in *Table 2*.

Table 2: The 5 FMC-based UD strength criteria

strains from FEA [Cun04, Cun11]

FF1 $Eff^{\parallel\sigma} = \breve{\sigma}_1 / \bar{R}^t_{\parallel} = \sigma^{\parallel\sigma}_{eq} / \bar{R}^t_{\parallel}$, $\breve{\sigma}_1 \cong \varepsilon^t_1 \cdot E_{\parallel}$ *

FF2 $Eff^{\parallel\tau} = -\breve{\sigma}_1 / \bar{R}^c_{\parallel} = +\sigma^{\parallel\tau}_{eq} / \bar{R}^c_{\parallel}$, $\breve{\sigma}_1 \cong \varepsilon^c_1 \cdot E_{\parallel}$

2 filament modes

IFF1 $Eff^{\perp\sigma} = [(\sigma_2+\sigma_3) + \sqrt{(\sigma_2-\sigma_3)^2 + 4\tau_{23}^2}]/2\bar{R}^t_{\perp} = \sigma^{\perp\sigma}_{eq} / \bar{R}^t_{\perp}$ ≡ Puck Mode A

IFF2 $Eff^{\perp\tau} = [(\frac{\mu_{\perp\perp}}{1-\mu_{\perp\perp}})\cdot(\sigma_2+\sigma_3) + \frac{1}{1-\mu_{\perp\perp}}\sqrt{(\sigma_2-\sigma_3)^2+4\tau_{23}^2}] / \bar{R}^c_{\perp} = +\sigma^{\perp\tau}_{eq} / \bar{R}^c_{\perp}$ 3 matrix modes

IFF3 $Eff^{\perp\parallel} = \{[\mu_{\perp\parallel}\cdot I_{23-5} + (\sqrt{\mu_{\perp\parallel}^2 \cdot I_{23-5}^2 + 4\cdot\bar{R}_{\perp\parallel}^2\cdot(\tau_{31}^2+\tau_{21}^2)^2}]/(2\cdot\bar{R}_{\perp\parallel}^3)\}^{0.5} = \sigma^{\perp\parallel}_{eq} / \bar{R}_{\perp\parallel}$

with $I_{23-5} = 2\sigma_2\cdot\tau_{21}^2 + 2\sigma_3\cdot\tau_{31}^2 + 4\tau_{23}\tau_{31}\tau_{21}$

The interaction of the five modes reads

$$Eff^m = (Eff^{\parallel\tau})^m + (Eff^{\parallel\sigma})^m + (Eff^{\perp\sigma})^m + (Eff^{\perp\tau})^m + (Eff^{\perp\parallel})^m = 1 .$$

A typical data range for the friction values is $0.05 < \mu_{\perp\parallel} < 0.3$, $0.05 < \mu_{\perp\perp} < 0.2$.

Due to mapping experience in the transition domains the interaction exponent is $2.5 < m < 3$. For reasons of simplicity the same value is applied for all interactions. Mind also here the Poisson effect: biaxial compression strains the filament without any external σ_1.

This microscopic failure is considered in the macroscopic strength criteria above.

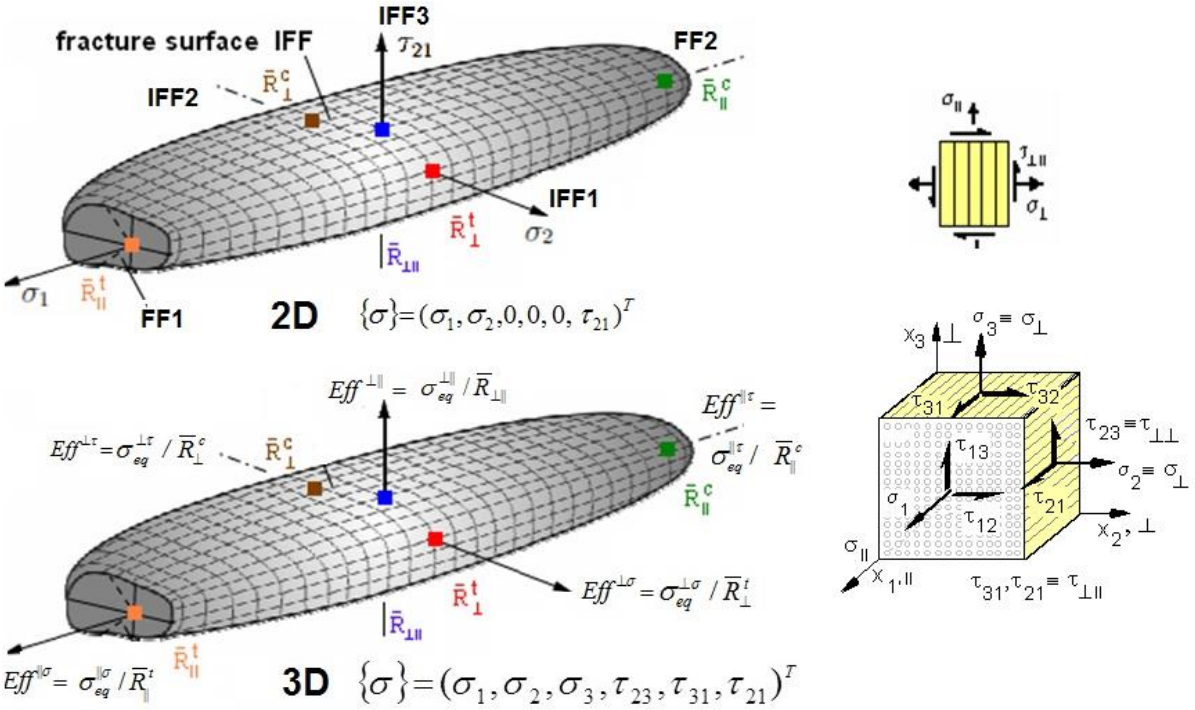

Figure 9: Fracture body of the UD materials Lamella, Sheet (tape)

The 3D fracture body above does not take joint effects of all the six stresses into account concerning a possible twofold failure occurrence $\sigma_3 \approx \sigma_2$. This is considered by an additional effort term which has the same effect as J_3 in the isotropic case.

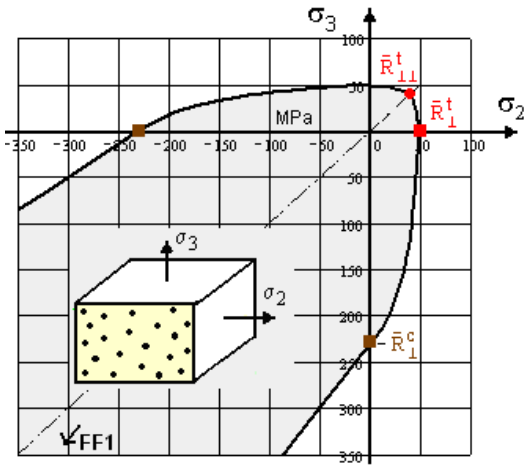

Figure 10: Twofold failure occurrence with UD materials

Conclusions

- A usual SFC just describes a 1-fold occurring failure mode (mechanism)
- A multi-fold occurrence of a failure with its joint probabilistic effects must be additionally considered in the formulas
- The 120°-located dents of the isotropic fracture failure body, as the probabilistic result of the *2-fold* acting of the same failure mode
- Determination of model parameters is to perform by mapping in each pure failure domain and of the interaction exponent *m* by determination in the transition zone between the modes
- Simple computation of the reserve factor *RF* for design verification is possible with consideration of the stochastic nature of the material properties

- Porous Concrete Stone: the fracture body is 120° rotational symmetric, fully non-circular and the dents - in contrast to Normal Concrete - are oppositely located in the $I_1<0$ domain to those in the $I_1>0$ domain. Or, the dents do not lie on the same meridian as with Normal Concrete
- UHPC: Due to redundancy effects ('healing' of the fracture inducing flaws) non-circularity (not round or circular) will reduce with increasing $p_{hyd.}$. For the pretty flawless UHPC - in comparison to Normal Concrete – this effect still holds however under the permitted much higher hydrostatic loading stresses a volume reduction effect overloads
- Lamella, Sheet: The fracture body is the well-known flattened 'cigar' of UD materials
- The Poisson effect, generated by a Poisson ratio *v (estimation > 0.2)*, may cause tensile failure under 2D compression, because concrete fractures under an internal axial tensile straining. Fibers in a UD lamina may – even - fracture under a 3D compression p_{hyd} of many thousands MPa.
- The FMC does not build on a material but on the material's solid deformation behaviour!.

This paper comprises results of the author's non-funded research work.

Literature most of the literature is uploaded on
carbon~connected.de/Group/CCeV.Fachinformationen/Mitglieder (open website, access after registration)

[Cun04] Cuntze R: *The Predictive Capability of Failure Mode Concept-based Strength Criteria for Multidirectional Laminates*. WWFE-I, Part B, Comp. Science and Technology 64 (2004), 487-516

[Cun10] Cuntze R: *Failure Mode-based Lifetime Prediction of Brittle behaving UD Laminas-composed Laminates*. NAFEMS Seminar Wiesbaden 2010, Nov. 10 – 11. Conference publication. 10 pages

[Cun13] Cuntze R: *Comparison between Experimental and Theoretical Results using Cuntze's 'Failure Mode Concept' model for Composites under Tri-axial Loadings - Part B of the WWFE-II*. Journal of Composite Materials, Vol.47 (2013), 893-924

[Cun14] Cuntze R: *The World-Wide-Failure-Exercises-I and –II for UD-materials – valuable attempts to validate failure theories on basis of more or less applicable test data*. SSMET 2014, Braunschweig, April 1 – 4, 2014, conference handbook

[Cun16a] Cuntze R: *Fracture failure surface of the foam Rohacell 71G*. 3. NAFEMS Regionalkonferenz, 25.-27. April, 2016. Berechnung und Simulatioion, 35 slides

[Cun16b] Cuntze R: *Introduction to the Workshop - from Design Dimensioning via Design Verification to Product Certification*. Experience Composites 16 (EC16), September 21 – 23, 2016, Augsburg. Extended Abstract in Symposium Abstracts. 10 pages

[Cun16c] Cuntze R: *Progress reached, in Static Design and Lifetime Estimation?* Mechanik-Kolloquium, TU-Darmstadt, December 21, 2016 (UD and isotropic materials, 150 slides)

[Kad13] Kaddour A and Hinton M: *Maturity of 3D failure criteria for fibre-reinforced composites: Comparison between theories and experiments*. Part B of WWFE-II, J. Compos. Materials 47 (6-7) (2013) 925–966.

[Pet16] Petersen E, Cuntze R and Huehne C: *Experimental Determination of Material Parameters in Cuntze's Failure-Mode-Concept -based UD Strength Failure Conditions.* Composite Science and Technology 134, (2016), 12-25

[VDI2014] VDI 2014: German Guideline, Sheet 3 *Development of Fibre-Reinforced Plastic Components, Analysis*. Beuth Verlag, 2006. (in German and English, author was convenor)

Definitions

Brittle material behavior: about $R^c / R^t > 3$

Cross sections of the fracture failure body (surface): (1) convex π-plane ≡ plane I_1 = constant ≡ hoop plane; (2) deviatoric plane = meridian planes (tensile, compressive, shear), may be not convex at $I_1 \rightarrow$ max I_1

Design verification: determination of the reserve factor *RF* on basis of a statistically reduced strength failure body with its spanning strengths

Equivalent stress σ_{eq} *(author's view):* (1) Equivalent (in German gleichwertig) to a multi-axial stress state combining the effects of those stresses that are active in a distinct failure mode. *Examples:* *von Mises equivalent stress: in the case of the associated 'shear yielding' failure mode and *maximum principal stress: in the case of a brittle 'tensile fracture' failure mode NF. (2) The uni-axial scalar σ_{eq}-value (in German termed 'Vergleichsspannung'= vergleichbar) can be compared to a mode-associated (uni-axial) strength *R* of the activated failure mode

Failure: structural part does not fulfil its functional requirements such as onset of yielding, brittle fracture, leakage, deformation limit, delamination size limit, frequency bound, heat flow is usually provided as a 'project-fixed Limit State of failure'.

Failure types: basically addressed are Normal Fracture (NF) and Shear Fracture (SF, under compression)

Mapping of a course of test data: average test data fit

Material: homogenized (macro-) model of the envisaged solid

Material stressing effort Eff = artificial technical term created together with QinetiQ, UK, during the World-Wide-Failure-Exercises (since 1991) in order to obtain an English expression for the German term Werkstoff-Anstrengung. Note: In non-linear analysis the computation must run up to a theoretical fracture loading at *Eff* = 100% in order to determine the required *RF*

Mode equivalent stress σ_{eq}^{mode}: mode–dedicated equivalent stress. The highest mode equivalent stress gives the designer a possibility where to turn the design screw

Reserve Factor RF: predicted failure load / (design factor of safety x Design Limit Load). If linear analysis is permitted the material reserve factor f_{RF} = strength / Design Stress will correspond to *RF*. A value higher than 1 would permit a loading increase

Strength R (resistance): fracture tensile stress $\sigma^{+}\equiv$ ultimate tensile strength R^t, ultimate compressive strength R^c

Strength failure condition SFC (criterion) *F*: mathematical formulation of the failure surface or failure body (subset of a failure theory to assess a 'multi-axial failure stress state in a critical location of the structural part). The SFCs may be roughly discriminated as (1) Global SFC: describes the full failure surface by one single equation capturing all existing failure modes such as Normal or Shear Fracture, (2) Modal SFC: describes each failure mode-associated part of the full failure surface by an equation. Failure at microscopic level must be considered in a macroscopic failure criterion.